

# Observability of triple top quark signal at Future Hadron Colliders

Ijaz Ahmed,<sup>1,\*</sup> Nazima Bi,<sup>2</sup> and M. S. Amjad<sup>3,†</sup>

<sup>1</sup>*Federal Urdu University of Arts, Science and Technology, Islamabad Pakistan*

<sup>2</sup>*Riphah International University, Sector I-14, Hajj Complex, Islamabad Pakistan*

<sup>3</sup>*National University of Technology (NUTECH), Sector I-12, Islamabad Pakistan*

## Abstract

The Standard Model cross-sections for the production of single top, top quark in pairs, triple-top quarks, and four top-quarks at three different centre of mass-energies i.e,  $\sqrt{s}=7, 10$  and  $14$  TeV at existing particle colliders as well as at Future Hadron Colliders are studied. A fully kinematic analysis with the optimized pre-selection cuts along with invariant mass reconstruction of top quarks is performed for triple-top production processes  $pp \rightarrow tttW, tttd, ttbt$  in presence of the SM background. All three signal processes are forced to decay in fully hadronic mode. The studies are performed for High Luminosity LHC (HL-LHC) at  $\sqrt{s}=14$  TeV and for High-Energy LHC (HE-LHC) at  $\sqrt{s}=27$  TeV. The signal to background ratio and signal significance of all signal and background processes are estimated for both the scenarios. It is found that the chances of signal observability at HE-LHC are higher than that at HL-LHC.

PACS numbers: 12.60.Fr, 14.80.Fd

Keywords: Charged Higgs, MSSM, LHC

---

\*Electronic address: Ijaz.ahmed@fuuast.edu.pk

†Electronic address: sohailamjad@nutech.edu.pk

## I. INTRODUCTION

Top-quark characteristics are one of the most important aspects of Standard Model (SM). It is also possible that top-quarks will play a key role in breaking electroweak symmetry, which is responsible for the masses of all fundamental particles. Top quarks have some unique properties including enormously large mass, and they could be a gateway to discovery new physics. Also owing to extremely short life time, bare quark properties could be studied as they decay before hadronization. Top-quarks have been observed to be produced singly through weak-interactions and in top-pairs through strong interactions [1, 2]. Due to the large mass, high collision energy is necessary to produce top-quarks. At LHC, a large number of top-quarks were produced at energy of 7 TeV and 8 TeV. As a result, top characteristics have been investigated in great detail and precision. These findings are consistent with the Standard Model's predictions for top quarks (SM). However, in BSM regime, there has been a limited focus on triple top, particularly. For example, [3] discusses the triple top in view of searches for scalar bosons. The authors propose that triple-top may be studied in the signature of three leptons plus three  $b$ -jets, as confirmation. They also argue that triple-top search at HL-LHC could conditionally cover full mass range up to 700 GeV. Also [4] includes the discussion on triple top in the context of FCNC induced by the  $Z'$  boson. The  $Z'$  boson produced in associated with single top quark and decaying to a  $t\bar{t}$  could decay to a triple top final state. This might become dominant as compared to single top under certain coupling conditions. However, there's also the possibility that it remains negligible under different coupling conditions.

Since its discovery [5] in Fermi-lab at Tevatron collider by the CDF and D0 Collaborations [6][7, 8], the top quark has remained the heaviest elementary particle. It completed the third-generation structure of the Standard Model (SM) and opened the top quark physics area [9]. The large mass of the top quark makes phenomenology so important as it is usually the most closely related to new physics proposals Beyond the Standard Model (BSM) [10]. In addition, it has a very short lifetime and decays without hadronisation [11], making top quark physics a unique playground to study a bare quark [12]. At the Tevatron and Large Hadron Collider (LHC), many properties of the top quark were studied, including the production mechanism, the basic properties such as mass and width, decay [13].

For both the Fermilab's Tevatron and CERN's Large Hadron Collider (LHC), top-pair and single top production have been extensively studied. Single top production is also of interest, especially for the Standard Model (SM)  $V_{tb}$  mixing element, and was observed at the Tevatron [14, 15]. Sev-

eral search programmes involve top-quark that is commonly considered sensitive to new physics on the TeV scale , e.g. top-quark pair production of opposite-sign or same-sign, single top-quark production, and four top-quark production. Unfortunately, triple top-quark production still does not receive too much attention. Of all the current top-quark-related physics search programs, the triple-top production is very special [16]. We measure single top, top pair, triple top and four top quark cross-sections at different mass energy centres in this paper and address the discovery potential of triple-top events at the Large Hadron Collider (LHC) and how new physics can significantly affect this channel.

## II. SINGLE TOP QUARK PRODUCTION

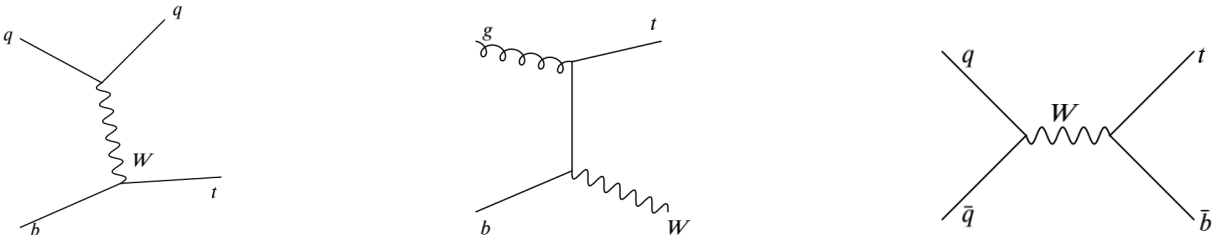


FIG. 1: Feynman diagram of single top quark production in SM: t-channel (left), W-associated production or tW-channel (center) and s-channel (right).

In Beyond the Standard Model (BSM), single top-quark production is also susceptible to physics including charged  $Wtb$  vertex structure, new gauge bosons, new heavy quarks, and top-quark neutral currents that change flavour [17, 18]. There are three different single top quark production modes at Large Hadron Collider (LHC) which are t-channel, s-channel and tW-channel production [19, 21]. Lowest order Feynman diagram for single top quark production through weak interaction are shown in Fig.1 .

## III. TOP PAIR PRODUCTION

The production of triple top quarks is a mixture of single top quarks and pairs [15]. According to the SM, the strong interactions generate top pairs at the Tevatron, as well as at the LHC [14] and single top quark production mostly through electroweak interaction with W-boson [19, 20]. Top -quark pairs are formed by quark-antiquark ( $q\bar{q} \rightarrow t\bar{t}$ ) annihilation and gluon-gluon fusion ( $gg \rightarrow t\bar{t}$ ). In the Tevatron collider, the first is the most dominant, while in the LHC, the second is

Process	No. of Diagrams	$\sqrt{s} = 7 \text{ TeV}$	$\sqrt{s} = 10 \text{ TeV}$	$\sqrt{s} = 14 \text{ TeV}$
$\sigma(t - \text{channel})[\text{fb}]$	4	$1.8039 \times 10^4$	$3.5832 \times 10^4$	$4.9552 \times 10^4$
$\sigma(s - \text{channel})[\text{fb}]$	4	$9.2312 \times 10^2$	$1.5027 \times 10^3$	$2.3140 \times 10^3$
$\sigma(tW - \text{channel})[\text{fb}]$	4	$2.9856 \times 10^3$	$6.5386 \times 10^3$	$1.5074 \times 10^4$

TABLE I: Cross section for single top quark production through weak interaction at Large Hadron Collider (LHC).

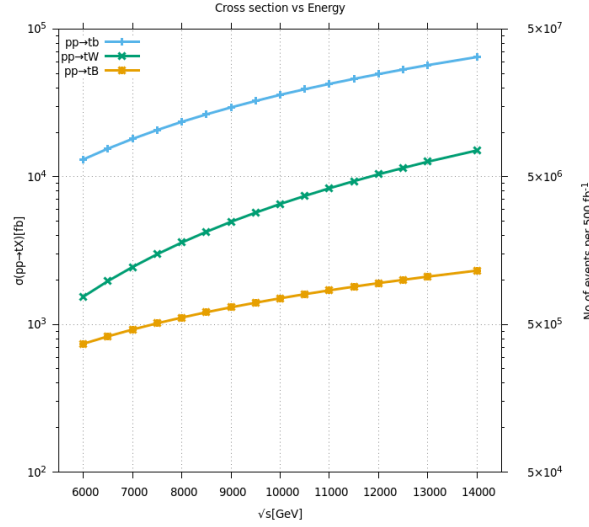


FIG. 2: Cross section for single top production in the Standard Model for different LHC center of mass energies.

dominant [9, 19, 22]. Fig.3 shows the Feynman diagram of the lowest order for top pair production by strong interaction.

Process	No. of Feynman Diagrams	$\sqrt{s} = 7 \text{ TeV}$	$\sqrt{s} = 10 \text{ TeV}$	$\sqrt{s} = 14 \text{ TeV}$
$\sigma(q\bar{q} \rightarrow t\bar{t})[\text{fb}]$	38	$5.6691 \times 10^3$	$1.0336 \times 10^4$	$1.7143 \times 10^4$
$\sigma(gg \rightarrow t\bar{t})[\text{fb}]$	3	$4.8952 \times 10^4$	$1.4287 \times 10^5$	$3.5331 \times 10^5$

TABLE II: Cross section for top quark pair production through strong interaction at LHC

We can see from Table II that the production of top quark pairs in LHC is much greater than that of Tevatron because of higher collision energy and higher luminosity [22].

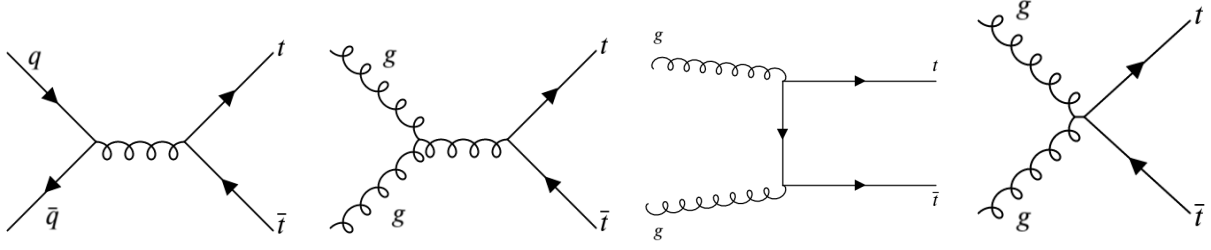


FIG. 3: Lowest order Feynman diagrams contributing to top quark pair production at Large Hadron Collider (LHC).

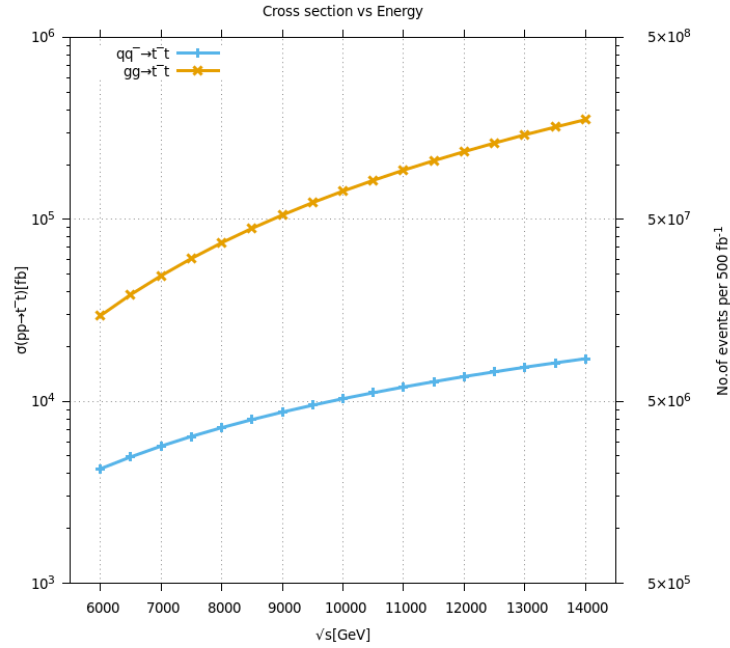


FIG. 4: Top quark pair production cross section for quark anti-quark annihilation and gluon-gluon fusion processes at Large Hadron Collider (LHC).

#### IV. TRIPLE TOP QUARK PRODUCTION

Triple top quark has three different production modes in the Standard Model (SM) at LHC [23]. The three production modes of triple top quark are  $pp \rightarrow 3t + W^\pm$ ,  $pp \rightarrow 3t + \bar{b}$  and  $pp \rightarrow 3t + d$ . [15]. Table III shows that triple top quark cross section is low. Due to its small cross section, triple top quark production is very rare [24].

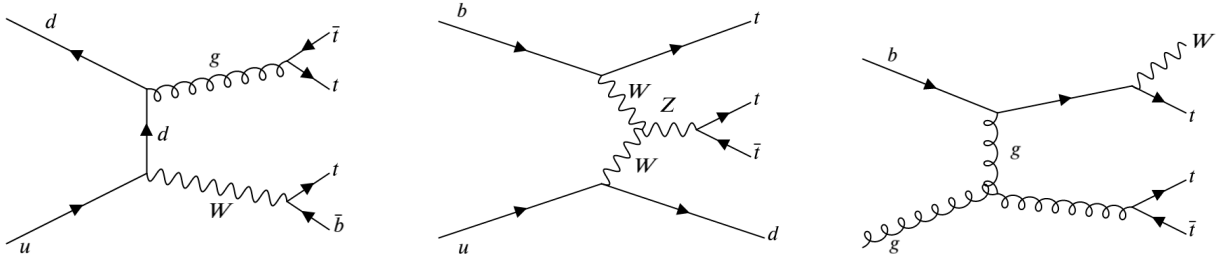


FIG. 5: Feynman diagrams for triple top quark production in Standard Model (SM) at Large Hadron Collider (LHC) corresponding to three processes.

Process	No. of Diagrams	$\sqrt{s} = 7 \text{ TeV}$	$\sqrt{s} = 10 \text{ TeV}$	$\sqrt{s} = 14 \text{ TeV}$
$\sigma(pp \rightarrow tt\bar{t} + W^-)[\text{fb}]$	118	$1.8039 \times 10^4$	$3.5832 \times 10^4$	$4.9552 \times 10^4$
$\sigma(pp \rightarrow tt\bar{t} + d)[\text{fb}]$	76	$9.2312 \times 10^2$	$1.5027 \times 10^3$	$2.3140 \times 10^3$
$\sigma(pp \rightarrow tt\bar{t} + \bar{b})[\text{fb}]$	36	$2.9856 \times 10^3$	$6.5386 \times 10^3$	$1.5074 \times 10^4$

TABLE III: Cross section for triple top quark production at LHC.

The triple top cross section is very small compared to the Standard Model (SM) prediction which makes it an interesting channel to study. The process  $pp \rightarrow tt\bar{t} + W^-$  has the larger cross-section as compared to other processes at different center of mass energies.

## V. FOUR TOP QUARK PRODUCTION

Four top quarks has two production modes quark anti-quark annihilation and gluon-gluon fusion. The gluon-gluon fusion process is dominant at LHC. The gluon-gluon fusion has a contribution of 90% and quark anti-quark annihilation of 10%. The cross-section of four top quarks production is around five orders of magnitude smaller than the top pair production and so it has yet to be observed [25].

Table IV shows the cross section for quark anti-quark annihilation ( $q\bar{q} \rightarrow t\bar{t}t\bar{t}$ ) and gluon-gluon fusion ( $gg \rightarrow t\bar{t}t\bar{t}$ ) at different center of mass energy for four top quark production.

FIG. 6: Cross section for triple top production in SM for different LHC center of mass energies.

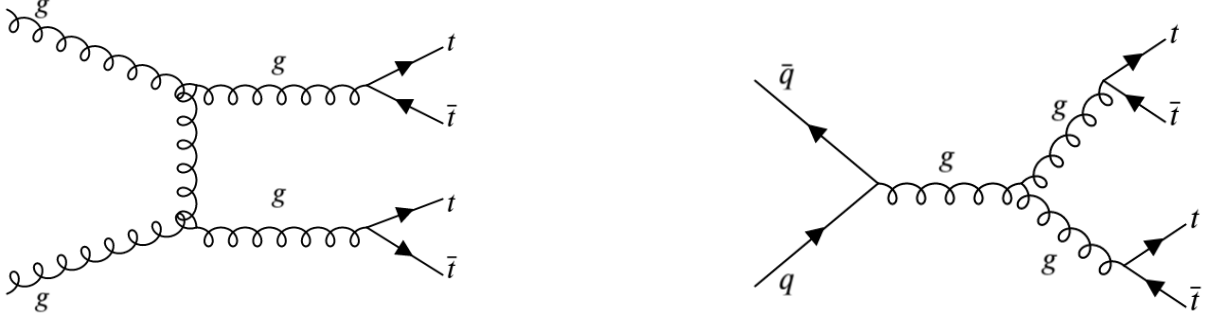


FIG. 7: Feynman diagrams for four top quark production in Standard Model (SM) at Large Hadron Collider (LHC) corresponding to quark anti-quark annihilation and gluon fusion processes.

Process	No. of Diagrams	$\sqrt{s} = 7 \text{ TeV}$	$\sqrt{s} = 10 \text{ TeV}$	$\sqrt{s} = 14 \text{ TeV}$
$\sigma(q\bar{q} \rightarrow t\bar{t}t\bar{t})[\text{fb}]$	54	$5.6691 \times 10^3$	$1.0336E \times 10^4$	$1.7143 \times 10^4$
$\sigma(gg \rightarrow t\bar{t}t\bar{t})[\text{fb}]$	54	$4.8952 \times 10^4$	$1.4287 \times 10^5$	$3.5331 \times 10^5$

TABLE IV: Cross section for four top quark production at Large Hadron Collider (LHC).

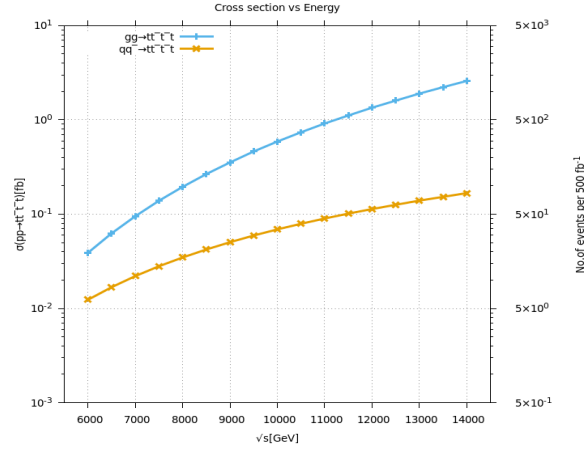


FIG. 8: Cross section for four top production in the Standard Model (SM) for different Large Hadron Collider (LHC) center of mass energies.

## VI. SIGNAL AND BACKGROUND PROCESSES

In this study, various scattering mechanisms are used as signals. The  $tt\bar{t}W$ ,  $tt\bar{t}\bar{b}$ , and  $tt\bar{t}d$  are scattering processes. All of these scattering mechanisms are generated by proton-proton collisions

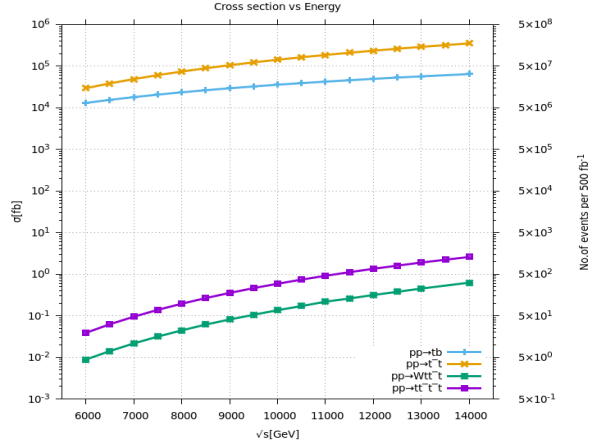


FIG. 9: Cross section for single, pair, triple and four top production in the (SM) for different LHC center of mass energies.

at  $\sqrt{s}=14$  TeV. In all of the triple-top signal processes, hadronic decay of the  $W$ -boson is taken into account. In the  $t\bar{t}W$ ,  $t\bar{t}b$ , and  $t\bar{t}d$  scattering processes, top-quark ( $t$ ) decays into  $W$ -boson and bottom quark ( $b$ ).  $W$  decays to produce light jets ( $u, d, c, s$ ). As a result, there are eleven jets in the final state of the scattering process  $t\bar{t}W$ , consisting of eight light jets and three  $b$ -jets.  $pp \rightarrow t\bar{t}W \rightarrow 4W^\pm + 3b\text{ jets} \rightarrow 8\text{ jets} + 3b\text{ jets}$ . There are ten jets in the final state of the scattering process  $t\bar{t}b$ , which includes six light jets and four  $b$ -quarks jets  $pp \rightarrow t\bar{t}b \rightarrow 3W^\pm + 4b\text{ jets} \rightarrow 6\text{ jets} + 4b\text{ jet}$ . Similarly, the  $t\bar{t}d$  scattering process produces ten jets, seven of which are light jets and three of which are  $b$ -jets  $pp \rightarrow t\bar{t}d \rightarrow 3W^\pm + 3b\text{ jets} \rightarrow 7\text{ jets} + 3b\text{ jets}$ .

The following background processes of SM with similar final state topologies are produced while analyzing these signal processes. In  $t\bar{t}Z$ ,  $t\bar{t}W^\pm$  and  $W^+W^-Z$ , top quark decays into  $W$  boson and  $b$  jet. When  $Z$  and  $W$  decay, they produce a pair of light jets. In  $pp \rightarrow t\bar{t}Z \rightarrow 6\text{ jets} + 2b\text{ jets}$ ,  $t\bar{t}W \rightarrow 6\text{ jets} + 2b\text{ jets}$  and in  $W^+W^-Z \rightarrow 6\text{ jets}$ .

## VII. EVENT SELECTION AND COLLIDER ANALYSIS

A complete analysis of three processes whose cross sections are presented in above section are studied. Three signal processes are explored where three top quarks are produced along with additional particle in each process and fully hadronic decay modes are selected. The parton density function is provided by LHAPDF 5.9.1 [27] with the version CTEQ 6.6. The background processes  $W^+W^-Z$ ,  $t\bar{t}W^\pm$ ,  $t\bar{t}Z$  are generated with calchep [28] with a kinematic preselection cut applied on jets as  $E_T^{\text{jets}} > 15$  GeV and  $|\eta| < 3.0$ , [29]. All the signal processes are also produced with Calchep.



$\sqrt{s}$ [TeV]	$t\bar{t}\bar{t}W$	$t\bar{t}\bar{t}b$	$t\bar{t}\bar{t}d$	$t\bar{t}h$	$t\bar{t}Z$	$t\bar{t}W$	$tWZ$	WWZ	$tZj$
[TeV]	fb	fb	fb	fb	fb	fb	fb	fb	fb
14	1.5	0.1	0.2	483	703	402	141	90	816
27	12.7	0.45	1.2	838	3329	1176	691	263	3142
100	352	3.5	13	11490	44800	6976	8970	1463	26380

TABLE V: Cross-sections of three signals and background processes are shown at three different energies using Next-to-Next Leading Order parton density function

The output of both these packages in Les Houches Event (LHE) format is used by PYTHIA8 for parton showering, gluon radiation, fragmentation and hadronization. PYTHIA calculates their relative efficiency as well. The HepMC v2.06.09 interface with PYTHIA is then used to record events. FastJet v3.3.4 is then coupled with PYTHIA for jet definition and reconstruction. The jet cone size is fixed at  $\Delta R = 0.4$ , where  $\Delta R = \sqrt{(\Delta\eta)^2 + (\Delta\phi)^2}$  is jet cone radius,  $\phi$  is azimuthal angle and  $\eta = -\ln \tan \theta / 2$  is pseudorapidity. The output is then analysed with ROOT v6.14.06. In this study, various scattering mechanisms are used as signals. The  $t\bar{t}\bar{t}W$ ,  $t\bar{t}\bar{t}b$ , and  $t\bar{t}\bar{t}d$  are scattering processes. All of these scattering mechanisms are generated by p-p collisions at  $\sqrt{s}=14$  TeV High Luminosity LHC (HL-LHC) and  $\sqrt{s}=27$  TeV center-of-mass energy at High Energy LHC (HE-LHC). In all of the triple-top signal processes, a hadronic decay of the W-boson is taken into account.

Various selection cuts are used to reduce background while keeping the signal. The chi-square method is used to reconstruct the physics objects in which we are interested. Several kinematic variables are plotted during entire analysis to examine the distributions of W bosons and top quark etc.

Jets are reconstructed using the Anti- $k_t$  technique with R and  $\Delta R$  set to 0.4 in this investigation.

Some of the jets in this mechanism extend beyond the cone size due to a variety of causes such as detector impairment, magnetic field influence, and material influence. All of these jets are sorted by  $p_T$  and the following kinematic cut on jets is applied.

$$P_T^{ljets} \geq 15 \text{ GeV and } |\eta| \leq 2.5$$

The selected jets are then tagged as either a b-jet or a light jet. In order to do this, we do  $\Delta R$

matching of jets with the parton level b- and c-quarks. Charm quarks are used to increase efficiency since their masses are closer to those of bottom quarks. The jets which are within  $\Delta R < 0.2$  are identified as b-jets and all the other jets which are farther away from b-quarks are identified as light jets. Once the tagging is done, we apply a multiplicity cut on jets. In  $t\bar{t}W$  analysis, there are eight light jets and three b jets so we only keep the events where we have

$$N_{ljets} \geq 8, N_{bjets} \geq 3$$

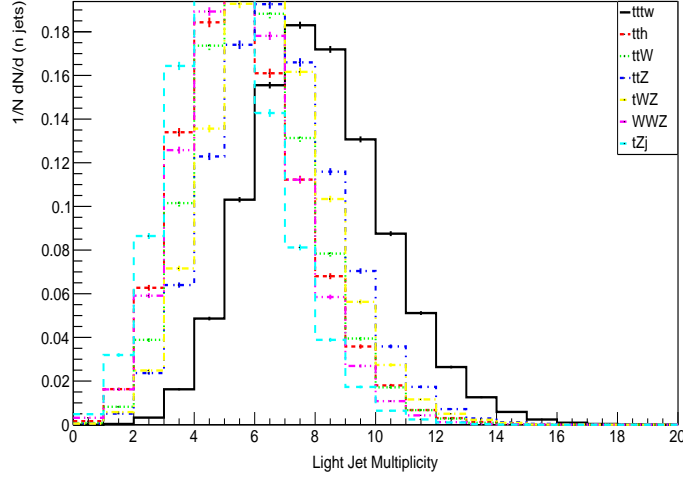


FIG. 10: The jet multiplicity distributions of both signal and background events are shown at  $\sqrt{s}=14$  TeV

Similarly, for  $t\bar{t}b$ , there are six light jets and for b jets so event selection cut becomes

$$N_{ljets} \geq 6, N_{bjets} \geq 4$$

and for process  $t\bar{t}d$

$$N_{ljets} \geq 7, N_{bjets} \geq 3$$

In figure 10 light jet multiplicity of signal processes with backgrounds are given. It can be seen almost 20 percent jets are passed through jets kinematic cut. Also it can be seen jet multiplicity of scattering processes is almost same. Distribution of pseudorapidity and transverse momentum of selected jets are also given in figure 12 and figure 13 respectively .

It can be seen from figure, prominent signals with b-jets. In case of  $t\bar{t}b$  scattering process four b-jets efficiency is in range of 50 percent. But in case of  $t\bar{t}d$  and  $t\bar{t}W$  it increases upto 75 percent to 80 percent. Presence of SM backgrounds as compare to signal is low. Figure 11 shows the distributions of b-jet multiplicities for various signals and backgrounds.

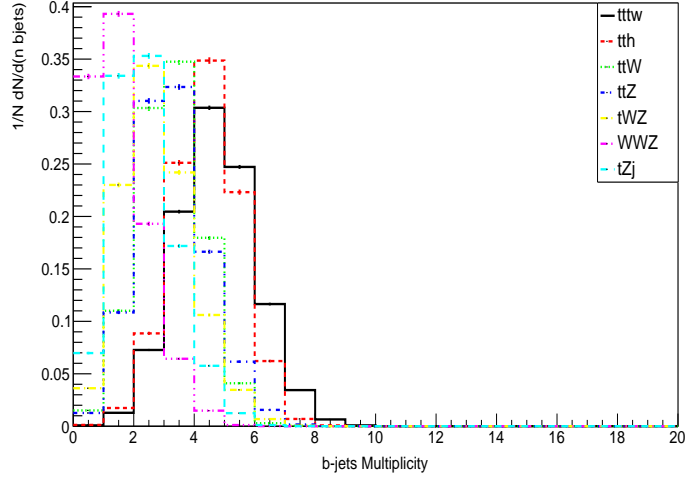


FIG. 11: The b-jets multiplicity distributions in both signal and background events

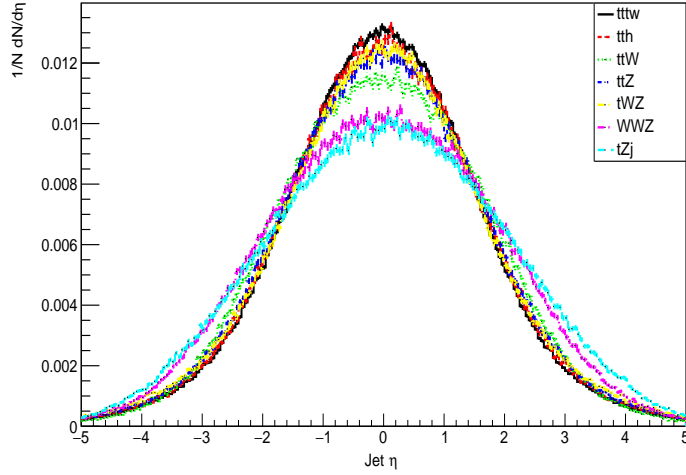


FIG. 12: Pseudorapidity distributions of signal and background selected jets at  $\sqrt{s}=14$  TeV

## VIII. RECONSTRUCTION OF INVARIANT MASSES

In particle physics, the invariant mass is defined as it's mass in the rest frame and is given as

$$m_0 c^2 = \left( \frac{E}{c} \right)^2 - |p|^2 \quad (1)$$

Set  $c = 1$  for convenience,

$$m_0 = (E)^2 - |p|^2 \quad (2)$$

After selecting desired events from randomly produced events. The reconstruction of invariant masses from decays product is the next step. First, the invariant mass of the W-boson is recon-

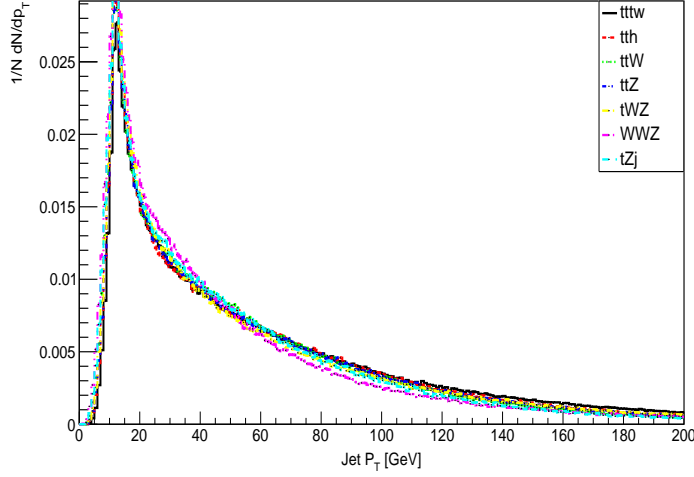


FIG. 13: Transverse momentum distributions of selected jets at  $\sqrt{s}=14$  TeV

structed. For this, all events having at least 8 jets for the  $tt\bar{t}W$  signal, 6 jets for the  $tt\bar{t}b$  signal, and 7 jets for the  $tt\bar{t}d$  signal are chosen, and the invariant mass is reconstructed using all possible light jets pairs using formula.

$$\mathbf{W}_{j_1 j_2} = \sqrt{(\mathbf{E}_{j_1} + \mathbf{E}_{j_2})^2 - (\mathbf{p}_{x_{j_1}} + \mathbf{p}_{x_{j_2}})^2 - (\mathbf{p}_{y_{j_1}} + \mathbf{p}_{y_{j_2}})^2 - (\mathbf{p}_{z_{j_1}} + \mathbf{p}_{z_{j_2}})^2} \quad (3)$$

## IX. CHI-SQUARE METHOD

The chi-square method is then used to reconstruct the physics object of interest with correct invariant mass. For reconstruction of W boson, we check the invariant mass of di-jet objects and chose the six jets that give the minimal value of chi-square defined as,

$$\chi_W^2 = \sum_{i=1}^3 \left( \frac{m_{i,jj} - m_W}{\sigma_{m,jj}} \right)^2 \quad (4)$$

where  $m_{i,jj}$  is the di-jet mass,  $m_W$  is the mass of W boson and  $\sigma_{m,jj}$  is the width of the di-jet mass distribution obtained from the parton matched jets. The events are only selected if the  $\chi_{W,min}^2 < 10$ . Once the W's are reconstructed, we again apply the same method to reconstruct top quark candidates using the selected b-jets and the reconstructed W's.

$$\chi_t^2 = \sum_{i=1}^3 \left( \frac{m_{i,jjb} - m_t}{\sigma_{m,jjb}} \right)^2 \quad (5)$$

where the light jets are the ones chosen to make W bosons,  $m_{i,jjb}$  is a tri-jet mass,  $m_t$  is the mass of top quark and  $\sigma_{m,jjb}$  is the width of tri-jet distribution. Once again, the event is only selected if  $\chi_{t,min}^2 < 10$ .

## X. EVENT SELECTION EFFICIENCIES

In this study, 80000 events are generated and combined for signal processing in order to improve simulation results on selected kinematical cuts. Then signal efficiency corresponding to each selection cut is computed and then at the end, total efficiency is calculated. Total efficiency corre-

Process	$t\bar{t}W$	$t\bar{t}Z$	$t\bar{t}W$	$t\bar{t}H$	$tWZ$	$tZj$	WWZ
$N_{ljets} \leq 8$	0.49	0.25	0.14	0.13	0.20	0.06	0.10
$N_{bjets} \leq 3$	0.86	0.38	0.34	0.76	0.20	0.08	0.017
$\chi_{W,min}^2 < 10$	0.87	0.87	0.85	0.86	0.85	0.80	0.78
$\chi_{t,min}^2 < 10$	0.89	0.85	0.89	0.91	0.78	0.81	0.62
Total Efficiency	0.32	0.07	0.037	0.08	0.02	0.003	0.001
K factor	-	1.27	1.24	1.21	-	-	-
Total Efficiency	0.32	0.09	0.045	0.097	0.02	0.003	0.001

TABLE VI: Efficiencies of signal  $t\bar{t}W$  and SM background process efficiencies at various kinematics and selection cuts.

sponds to nine jet final states obtained at the end of the simulation, which consists of six light jets coming from three W-boson decay and b-jets resulting from top-quark decay. All these efficiency are calculated at centre of mass energy 14 TeV . All these efficiencies are mentioned in Tabs VI, VII and VIII. The QCD k-factor values of  $t\bar{t}Z$ ,  $t\bar{t}W$ ,  $t\bar{t}H$  are written in table VI, which are calculated by taking the ratio of  $\sigma_{NLO}/\sigma_{LO}$  of given process reported in [30], [31] and [32] respectively. It can be seen that the efficiency of light jets for various kinematical cuts ranges from 15 percent to 26 percent for signals. In addition, the efficiency of b-jet production ranges from 50 percent to 80 percent for signals. The total efficiency of top-mass reconstruction and nine jet final states for the specified signal situation is very low, ranging from 6 percent to 8 percent.

Process	$t\bar{t}\bar{b}$	$t\bar{t}Z$	$t\bar{t}W$	$t\bar{t}H$	$tWZ$	$tZj$	WWZ
$N_{ljets} \leq 6$	0.61	0.62	0.48	0.41	0.58	0.30	0.40
$N_{bjets} \leq 4$	0.60	0.14	0.12	0.48	0.066	0.014	0.003
$\chi^2_{W,min} < 10$	0.87	0.86	0.84	0.86	0.83	0.78	0.74
$\chi^2_{t,min} < 10$	0.84	0.83	0.87	0.88	0.79	0.75	0.75
Total Efficiency	0.27	0.063	0.041	0.15	0.025	0.003	0.001
K factor	-	1.27	1.24	1.21	-	-	-
Total Efficiency	0.27	0.08	0.050	0.18	0.025	0.003	0.001

TABLE VII: Signal  $t\bar{t}\bar{b}$  SM background process efficiencies at various kinematics and selection cuts.

Process	$t\bar{t}d$	$t\bar{t}Z$	$t\bar{t}W$	$t\bar{t}H$	$tWZ$	$tZj$	WWZ
$N_{ljets} \leq 7$	0.47	0.42	0.28	0.26	0.38	0.15	0.22
$N_{bjets} \leq 3$	0.81	0.40	0.37	0.78	0.22	0.088	0.02
$\chi^2_{W,min} < 10$	0.96	0.97	0.97	0.98	0.96	0.95	0.93
$\chi^2_{t,min} < 10$	0.706	0.69	0.76	0.79	0.60	0.56	0.55
Total Efficiency	0.26	0.12	0.081	0.16	0.049	0.007	0.002
K factor	-	1.27	1.24	1.21	-	-	-
Total Efficiency	0.26	0.15	0.1	0.19	0.049	0.007	0.002

TABLE VIII: Signal  $t\bar{t}d$  and SM background process efficiencies at various kinematics and selection cuts.

## XI. SIGNAL SIGNIFICANCE

To test the observability of the triple top mass at various kinematical cuts, signal significance is calculated for each triple top-mass distribution shown in the figures from 6.31 to 6.39 by incorporating the total number of signal and background candidate masses within the selected mass limit.

Signal significance is calculated using integrated luminosity  $3000 \text{ fb}^{-1}$ . The computed results, which include signal  $S$  and background  $B$  of candidate masses, signal to background ratio  $S/B$ , and signal significance  $S/\sqrt{B}$  at  $\sqrt{s} = 14 \text{ TeV}$  and  $27 \text{ TeV}$ , are shown in the table X, IX. The figure 14

FIG. 14: Candidate mass distribution of triple top at integrated luminosity  $3[ab^{-1}]$  at  $\sqrt{s} = 14 \text{ TeV}$ .

shows that at  $14 \text{ TeV}$ , the background is more dominant than the signal. As a result, the signal is not detectable because the cross-section of the triple top is very low even at  $14 \text{ TeV}$ .

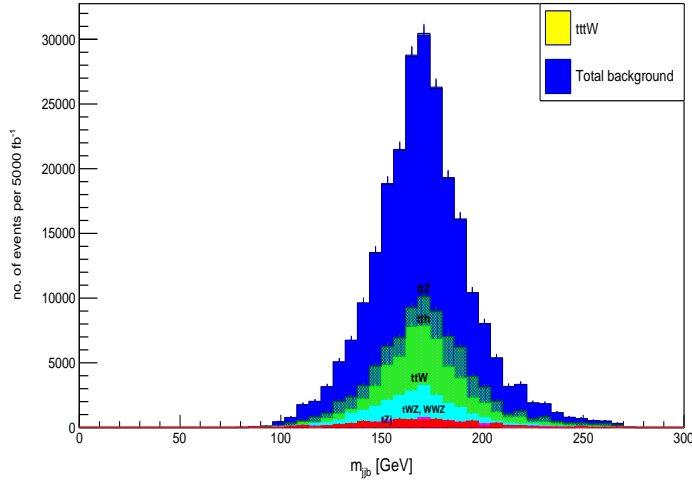


FIG. 15: The signal and background samples are normalized to the real number of events obtained at  $5000 \text{ fb}^{-1}$

Because the production process  $tt\bar{t}W$  has the largest cross-section for both  $\sqrt{s} = 14 \text{ TeV}$  and  $\sqrt{s} = 27 \text{ TeV}$ , its  $S/B$  ratio is 1. As a result, triple top has observability chances with the production process  $tt\bar{t}W$  for both LHC and HE-LHC. The other two process have very low cross-section and signal significance.

## XII. CONCLUSION

In the scope of SM, various channels of triple top quark generation are considered. This analysis of triple-top production shows that it has a very low cross-section when compared to other top-quark production modes. The mass of triple-top is reconstructed using hadronic decay of the top-quark at  $\sqrt{s} = 14 \text{ TeV}$ . The calculation of signal to background ratio and signal significance

Signal process	Mass window		Total	no. of	S/B	Optimized
	Lower limit	Upper limit	Efficiency	Events		$S/\sqrt{B}$
$t\bar{t}W^+$ Signal	186	294	0.11	282	0.003	1.045
Total Background	186	294		73143		
$t\bar{t}b$ Signal	280	287	0.0002	0.03	0.0001	0.002
Total Background	280	287		325		
$t\bar{t}d$ Signal	280	287	0.0003	0.12	0.0003	0.006
Total Background	280	287		403		

TABLE IX: Signal to background ratio and signal significance values obtained for three different triple top production processes with maximum Integrated luminosity  $5000 \text{ fb}^{-1}$  at HL-LHC ( $\sqrt{s}=14 \text{ TeV}$ ) .

Signal process	Mass window		Total	no. of	S/B	Optimized
	Lower limit	Upper limit	Efficiency	Events		$S/\sqrt{B}$
$t\bar{t}W^+$ Signal	280	287	0.0001	2.27	0.003	0.1
Total Background	280	287		628		
$t\bar{t}b$ Signal	280	287	0.0003	0.22	0.0002	0.006
Total Background	280	287		1441		
$t\bar{t}d$ Signal	248	296	0.0002	0.03	0.001	0.007
Total Background	248	296		24		

TABLE X: Signal to background ratio and signal significance values obtained for three different triple top production processes with maximum Integrated luminosity  $5000 \text{ fb}^{-1}$  at HE-LHC ( $\sqrt{s}=27 \text{ TeV}$ ) .

clearly shows that at  $\sqrt{s}=14 \text{ TeV}$  and  $\sqrt{s}=27 \text{ TeV}$ , not all signal scenarios are observable. Only  $t\bar{t}W$  has a signal to background ratio of one. At LHC background are dominant and signal is not visible because of very low cross-section. Due to the low SM rate, it is conceivable to explore for contributions that are beyond the scope of SM (BSM), which may improve the cross section. Specific computations, however, are required to study actual BSM aspects.

- 
- [1] Wicke, Daniel Single and double top quark production at the Tevatron. In *arXiv preprint arXiv:1006.1275*, 2010.
- [2] Gouz, Yu P and Slabospitsky, SR Double top production at hadronic colliders. In *Physics Letters B*,



- 1999.
- [3] Masaya Kohda, Tanmoy Modak, Wei-Shu Hou Searching for new scalar bosons via triple-top signature in  $cg \rightarrow tS^0 \rightarrow tt\bar{t}$  Phys.Lett. B776 (2018) 379-384
  - [4] Sungwoong Cho, P. Ko, Jungil Lee, Yuji Omura, Chaehyun Yu Top FCNC induced by a  $Z'$  boson Phys. Rev. D 101, 055015 (2020)
  - [5] Gomez, B and Mooney, P and Negret, JP and Roldan, JMR and Fein, D and Forden, GE and James, E and Johns, K and Markosky, L and Milder, A and others Observation of the top quark. In *Physical Review Letters*, 1995.
  - [6] Chakraborty, Dhiman and Konigsberg, Jacobo and Rainwater, David Top-quark physics In *Annual Review of Nuclear and Particle Science*, 2003.
  - [7] Bärnreuther, Peter Top quark pair production at the LHC, 2012.
  - [8] Abachi, Shahriar and Abbott, B and Abolins, M and Acharya, Bannanje Sripath and Adam, I and Adams, DL and Adams, M and Ahn, S and Aihara, H and Alitti, J and others Observation of the top quark. In *Physical review letters*, 1995.
  - [9] Martin Beneke, Ilias Efthymiopoulos, Michelangelo L Mangano, J Womersley, A Ahmadov, G Azuelos, U Baur, A Belyaev, EL Berger, W Bernreuther, et al. Top quark physics. *arXiv preprint hep-ph/0003033*, 2000.
  - [10] Giammanco, Andrea Single top quark production at the LHC. In *Reviews in Physics*, 2016.
  - [11] Bruscino, Nello and ATLAS Collaboration and others. Top quark physics with the ATLAS detector: recent highlights. In *Physica Scripta*, 2020.
  - [12] Déliot, Frédéric and Van Mulders, Petra Top quark physics at the LHC. author=Déliot, Frédéric and Van Mulders, Petra, In *Comptes Rendus. Physique*, 2020.
  - [13] Young, Christopher. Top Quark Properties from ATLAS, 2020.
  - [14] Incandela, Joseph R and Quadt, Arnulf and Wagner, Wolfgang and Wicke, Daniel Status and prospects of top-quark physics. In *Progress in Particle and Nuclear Physics*, 2009.
  - [15] Barger, Vernon and Keung, Wai-Yee and Yencho, Brian Triple-top signal of new physics at the LHC. In *Physics Letters B*, 2010.
  - [16] Cao, Qing-Hong and Chen, Shao-Long and Liu, Yandong and Wang, Xiao-Ping. What can we learn from triple top-quark production? In *Physical Review D*, 2019.
  - [17] Tait, Tim MP and Yuan, C-P Single top quark production as a window to physics beyond the standard model. In *Physical Review D*, 2000.
  - [18] ATLAS collaboration and others Observation of the associated production of a top quark and a  $Z$  boson in pp collisions at  $\sqrt{s} = 13$  TeV with the ATLAS detector. *Journal of High Energy Physics*, 2020.
  - [19] Bernreuther, Werner Top-quark physics at the LHC. I *Journal of Physics G: Nuclear and Particle Physics*, 2008.
  - [20] Abazov, VM and Abbott, B and Abolins, M and Acharya, Bannanje Sripath and Adams, M and Adams, T and Aguilo, E and Ahsan, M and Alexeev, GD and Alkhazov, G and others. Observation of

- single top-quark production. In *Physical review letters*, 2009.
- [21] Kevin Kröninger, Andreas B Meyer, and Peter Uwer. Top-quark physics at the lhc. In *The Large Hadron Collider*, pages 259–300. Springer, 2015.
  - [22] Han, Tao The ”top priority” at the LHC. In *Perspectives on LHC Physics*, 2008.
  - [23] Boos, Eduard and Dudko, Lev Triple top quark production in Standard Model In *arXiv preprint arXiv:2107.07629*, 2021.
  - [24] Khanpour, Hamzeh Probing top quark FCNC couplings in the triple-top signal at the high energy LHC and future circular collider In *Nuclear Physics B*, 2020.
  - [25] CMS collaboration and others Search for standard model production of four top quarks in proton-proton collisions at sqrt (s)= 13 TeV *arXiv preprint arXiv:1702.06164*, 2017.
  - [26] Sirunyan, Albert M and Tumasyan, Armen and Adam, Wolfgang and Asilar, E and Bergauer, Thomas and Brandstetter, Johannes and Brondolin, Erica and Dragicevic, Marko and Erö, Janos and Flechl, Martin and others. Search for standard model production of four top quarks in proton–proton collisions at s= 13 TeV. In *Physics Letters B*, 2017.
  - [27] Whalley, MR and Bourilkov, D and Group, RC The Les houches accord PDFs (LHAPDF) and LHAGLUE. In *arXiv preprint hep-ph/0508110*, 2005.
  - [28] Belyaev, Alexander and Christensen, Neil D and Pukhov, Alexander CalcHEP 3.4 for collider physics within and beyond the Standard Model. In *Computer Physics Communications*, 2013.
  - [29] Sjöstrand, Torbjörn and Mrenna, Stephen and Skands, Peter A brief introduction to PYTHIA 8.1 In *Computer Physics Communications*, 2008.
  - [30] Giuseppe Bevilacqua, Heribertus Bayu Hartanto, Manfred Kraus, Jasmina Nasufi and Malgorzata Worek NLO QCD corrections to full off-shell production of  $t\bar{t}Z$  including leptonic decays. J. High Energy Phys. 08(2022) 060,
  - [31] John M. Campbell & R. Keith Ellis  $t\bar{t}W^\pm$  production and decay at NLO. J. High Energy Phys. 07(2012) 052,
  - [32] Daniel Stremmer & Malgorzata Worek Production and decay of the Higgs boson in association with top quarks. J. High Energy Phys. 02(2022) 196,